fungi establish an intracellular life style and turned these rhizobia from free-living bacteria into nitrogen-fixing endosymbionts. However, although the endomycorrhizal symbiosis is widespread in the plant kingdom only very few plant lineages, namely legumes and *Parasponia*, have recruited this mechanism for the rhizobial nodule symbiosis. Studies on the constraints underlying this evolutionary event in *Parasponia* can provide insight into whether and how this nitrogen-fixing symbiosis can be transferred to other nonlegumes.

References and Notes

1. V. Gewin, *Nature* **466**, 552 (2010).
2. M. J. Trinick, *Nature* **244**, 459 (1973).
3. A. D. L. Akkermans, S. Abdulkadir, M. J. Trinick, *Nature* **274**, 190 (1978).
4. K. J. Sytsma *et al*., *Am. J. Bot.* **89**, 1531 (2002).
5. G. Webster, P. R. Poulton, E. Cocking, M. R. Davey, *J. Exp. Bot.* **46**, 1131 (1995).
6. K. Pawlowski, T. Bisseling, *Plant Cell* **8**, 1899 (1996).
7. J. Sprent, *J. Exp. Bot.* **59**, 1081 (2008).
8. D. J. Marvel, J. G. Torry, F. M. Ausubel, *Proc. Natl. Acad. Sci. U.S.A.* **84**, 1319 (1987).
9. E. Limpens *et al*., *Science* **302**, 630 (2003); 10.1126/science.1090074.
10. S. Radutoiu *et al*., *Nature* **425**, 585 (2003).
11. J. F. Arrighi *et al*., *Plant Physiol.* **142**, 265 (2006).
12. S. Radutoiu *et al*., *EMBO J.* **26**, 392 (2007).
13. K. Markmann, M. Parniske, *Trends Plant Sci.* **14**, 77 (2009).
14. G. E. D. Oldroyd, M. J. Harrison, U. Paszkowski, *Science* **324**, 753 (2009).
15. S. Kosuta *et al*., *Proc. Natl. Acad. Sci. U.S.A.* **105**, 9823 (2008).
16. X. C. Zhang *et al*., *Plant Physiol.* **144**, 623 (2007).
17. X. C. Zhang, S. B. Cannon, G. Stacey, *BMC Evol. Biol.* **9**, 623 (2009).
18. S. G. Pueppke, W. J. Broughton, *Mol. Plant Microbe Interact.* **12**, 293 (1999).
19. Materials and methods are available as supporting material on *Science* Online.
20. C. Gleason *et al*., *Nature* **441**, 1149 (2006).
21. L. Tirichine *et al*., *Nature* **441**, 1153 (2006).
22. H. Zhu, B. K. Riely, N. J. Burns, J. M. Ane, *Genetics* **172**, 2491 (2006).
23. G. V. Lohmann *et al*., *Mol. Plant Microbe Interact.* **23**, 510 (2010).
24. S. K. Gomez *et al*., *BMC Plant Biol.* **9**, 10 (2009).
25. S. B. Cannon *et al*., *PLoS One* **5**, e11630 (2010).
26. L. Moulin, A. Munive, B. Dreyfus, C. Boivin-Masson, *Nature* **411**, 948 (2001).

27. We thank W. Broughton for NGR234; E. James, P. Hadobas, and T. J. Higgens for *Parasponia* seeds; P. van Dijk for flow cytometry; and J. Talag and W. Golser for BAC library construction. This research is funded by the Dutch Science Organization (Nederlandse Organisatie voor Wetenschappelijk Onderzoek) (VIDI 864.06.007).

Supporting Online Material

www.sciencemag.org/cgi/content/full/science.1198181/DC1
Materials and Methods
Figs. S1 to S16
References

23 September 2010; accepted 13 December 2010
Published online 23 December 2010;
10.1126/science.1198181

The Antiproliferative Action of Progesterone in Uterine Epithelium Is Mediated by Hand2

Quanxi Li,[1] Athilakshmi Kannan,[1] Francesco J. DeMayo,[2] John P. Lydon,[2] Paul S. Cooke,[1] Hiroyuki Yamagishi,[3] Deepak Srivastava,[4] Milan K. Bagchi,[5]* Indrani C. Bagchi[1]*

During pregnancy, progesterone inhibits the growth-promoting actions of estrogen in the uterus. However, the mechanism for this is not clear. The attenuation of estrogen-mediated proliferation of the uterine epithelium by progesterone is a prerequisite for successful implantation. Our study reveals that progesterone-induced expression of the basic helix-loop-helix transcription factor Hand2 in the uterine stroma suppresses the production of several fibroblast growth factors (FGFs) that act as paracrine mediators of mitogenic effects of estrogen on the epithelium. In mouse uteri lacking Hand2, continued induction of these FGFs in the stroma maintains epithelial proliferation and stimulates estrogen-induced pathways, resulting in impaired implantation. Thus, Hand2 is a critical regulator of the uterine stromal-epithelial communication that directs proper steroid regulation conducive for the establishment of pregnancy.

A sequential and timely interplay of the steroid hormones 17β-estradiol (E) and progesterone (P) regulates critical uterine functions during the reproductive cycle and pregnancy (*1*–*3*). Whereas E drives uterine epithelial proliferation in cycling females, P counteracts E-induced endometrial hyperplasia. In mice, preovulatory ovarian E stimulates uterine epithelial growth and proliferation on days 1 and 2 of pregnancy (*1*). However, starting on day 3, P produced by the corpora lutea terminates E-mediated epithelial proliferation. In response to P, epithelial cells exit from the cell cycle and enter a differentiation pathway to acquire the receptive state that supports embryo implantation on day 4 of pregnancy (*4*–*6*). To identify the P-regulated pathways that underlie the implantation process, we had previously examined alterations in mouse uterine mRNA expression profiles in the periimplantation period in response to RU-486 (mifepristone), a well-characterized progesterone receptor (PR) antagonist (*7*). Our results identified *Hand2*, a critical regulator of morphogenesis in a variety of tissues (*8*, *9*), as a potential PR-regulated gene. Real-time polymerase chain reaction (PCR) confirmed that the expression of Hand2 mRNA was greatly reduced in the uteri of RU-486–treated mice (*10*) (fig. S1A). The expression of Hand2 protein, localized exclusively in the uterine stroma, was also abolished after RU-486 treatment (fig. S1B), which indicated that PR controls Hand2 expression in the mouse uterus during early pregnancy.

To further confirm P regulation of *Hand2*, ovaries were removed from nonpregnant mice, and then these animals were injected with either vehicle or P. We observed intense nuclear expression of Hand2 protein in uterine stromal cells after P treatment. Similar treatment of PR-null females showed no induction of Hand2 protein (Fig. 1A). These results established that P induces Hand2 expression in the uterine stroma. Consistent with its regulation by P, Hand2 expression was observed in the stromal cells underlying the luminal epithelium on days 3 and 4 of pregnancy (Fig. 1B).

To investigate the function of *Hand2* in the uterus, we created a conditional knockout of this gene in the adult uterine tissue. Crossing of mice harboring the "floxed" *Hand2* gene ($Hand2^{f/f}$) with PR-Cre mice (in which Cre recombinase was inserted into the PR gene) generated $Hand2^{d/d}$ mice in which the *Hand2* gene is deleted selectively in cells expressing PR. As shown in fig. S2, *Hand2* expression was successfully abrogated in uteri of $Hand2^{d/d}$ mice. A breeding study demonstrated that $Hand2^{d/d}$ females are infertile (table S1). An analysis of the ovulation and fertilization in $Hand2^{f/f}$ and $Hand2^{d/d}$ females revealed no significant difference in either the number or the morphology of the embryos recovered from their uteri (fig. S3, A and B). The serum levels of P and E were comparable in $Hand2^{f/f}$ and $Hand2^{d/d}$ females on day 4 of pregnancy, which indicated normal ovarian function (fig. S3, C and D).

We next examined embryo attachment to the uterine epithelium by using the blue dye assay, which assesses increased vascular permeability at implantation sites. $Hand2^{f/f}$ mice displayed distinct blue bands, indicative of implantation sites on day 5 of pregnancy (fig. S4). In contrast, none of the $Hand2^{d/d}$ females showed any sign of implantation. Implanted embryos with decidual swellings were also absent in $Hand2^{d/d}$ uteri on days 6 and 7 of pregnancy. Histological analysis of $Hand2^{f/f}$ females on day 5 of pregnancy

[1]Department of Comparative Biosciences, University of Illinois Urbana/Champaign, Urbana, IL 61820, USA. [2]Department of Molecular and Cellular Biology, Baylor College of Medicine, Houston, TX 77030, USA. [3]Keio University School of Medicine, Tokyo 160-8582, Japan. [4]The Gladstone Institute of Cardiovascular Disease, University of California, San Francisco, CA 94158, USA. [5]Department of Molecular and Integrative Physiology, University of Illinois Urbana/Champaign, Urbana, IL 61820, USA.

*To whom correspondence should be addressed. E-mail: ibagchi@illinois.edu (I.C.B.); mbagchi@life.illinois.edu (M.K.B.)

showed, as expected, a close contact of embryonic trophectoderm with uterine luminal epithelium (Fig. 1C, a and b). In contrast, in *Hand2*$^{d/d}$ uteri, blastocysts remained unattached in the lumen (Fig. 1C, c and d). These results suggested that, in the absence of Hand2 expression in the stroma, the luminal epithelium fails to acquire competency for embryo implantation.

In mice, the window of uterine receptivity coincides with the P-mediated down-regulation of ER activity in uterine luminal epithelium (*5*, *6*). The levels of PR and estrogen receptor α (ERα) proteins in the luminal epithelium or stroma of *Hand2*$^{d/d}$ uteri were comparable to those of *Hand2*$^{f/f}$ controls (fig. S5). An examination of the phosphorylation of ERα at serine 118, indicative of its transcriptionally active state (*11*), revealed a sharp reduction of this modification in the luminal epithelial cells of *Hand2*$^{f/f}$ uteri on days 3 and 4 of pregnancy (fig. S6, a to d). In contrast, an increase in ERα phosphorylation was evident on these days in luminal epithelium of *Hand2*$^{d/d}$ uteri (fig. S6, e to h).

Consistent with this increase in ER transcriptional activity, expression of mRNAs corresponding to mucin 1 (*Muc-1*) and lactoferrin (*Lf*), well-characterized E-responsive genes in uterine epithelium (*12*), was significantly elevated in the *Hand2*-null uterus on day 4 of pregnancy (Fig. 2A). In contrast, the expression of *Ihh* (*13*), *Alox15* (*7*), and *Irg1* (*7*), which are known P-responsive genes in uterine epithelium, remained unaltered in *Hand2*$^{d/d}$ uteri (fig. S7). In addition, the mRNA levels of *Hoxa10*, a P-regulated stromal factor (*3*), and *Nr2f2*, a downstream target of *Ihh* in the uterine stroma (*13*), were unaffected in the uteri of *Hand2*$^{d/d}$ mice. However, the expression of leukemia inhibitory factor (*Lif*), a glandular factor that regulates uterine receptivity (*2*), was significantly reduced in *Hand2*$^{d/d}$ uteri (fig. S8).

Down-regulation of Muc-1 in the luminal epithelium is indicative of a receptive uterus (*12*). In contrast, persistent Muc-1 expression impairs acquisition of uterine receptivity and embryo implantation. On days 4 and 5 of gestation, a marked reduction in Muc-1 level was seen in uterine epithelia of *Hand2*$^{f/f}$ mice, consistent with the attainment of receptive status (fig. S9). However, Muc-1 expression persisted in uteri of *Hand2*$^{d/d}$ mice at the time of implantation. Thus, elevated epithelial ER signaling led to increased expression of Muc-1 and corresponded to disrupted uterine receptivity and implantation failure in *Hand2*$^{d/d}$ mice.

In normal pregnant uteri, the receptive state is also marked by a cessation in epithelial cell proliferation before implantation (*1*, *2*). As expected, in *Hand2*$^{f/f}$ mice, Ki-67, a cell proliferation marker, was undetectable in the uterine epithelium as it attains receptive status on day 4 of pregnancy (Fig. 2B, a). *Hand2*$^{d/d}$ uteri, on the other hand, exhibited robust Ki-67 expression in the luminal epithelium, which indicated sustained epithelial cell proliferation in the absence of *Hand2* (Fig. 2B, b).

The persistent proliferative state of uterine epithelium in the *Hand2*$^{d/d}$ mice raised the possibility that stromal expression of Hand2 mediates P action that opposes E-mediated epithelial proliferation. Administration of E to ovariectomized *Hand2*$^{f/f}$ and *Hand2*$^{d/d}$ mice led to robust uterine epithelial proliferation (Fig. 2C, a and b). Treatment with P alone induced proliferation exclusively in the uterine stromal cells of both genotypes (Fig. 2C, c and d). In *Hand2*$^{f/f}$ mice pretreated with P, administration of E showed no proliferative activity in the epithelium, which suggested a complete blockade of E-dependent proliferation by P. Under similar treatment conditions, *Hand2*$^{d/d}$ uteri exhibited a marked E-induced epithelial proliferation, indicating an absence of antiproliferative effects of P on the uterine epithelium (Fig. 2C, e and f). These results established Hand2 as a critical mediator of the actions of P in the stroma that inhibit E-dependent epithelial proliferation.

To identify downstream target(s) of Hand2 in the uterus, we performed gene expression profiling of uterine stromal cells isolated from *Hand2*$^{f/f}$ and *Hand2*$^{d/d}$ mice on day 4 of pregnancy. This study revealed elevated expression of mRNAs corresponding to several members of the fibroblast growth factor family (FGFs)—namely, *Fgf1*, *Fgf2*, *Fgf9*, and *Fgf18*—in uterine stroma of *Hand2*$^{d/d}$ mice. Real-time PCR confirmed the induction of *Fgf1*, *Fgf9, Fgf2*, and *Fgf18* mRNAs in uterine stromal cells of *Hand2*$^{d/d}$ mice (Fig. 3A). The expression of *Hbegf* mRNA, encoding the heparin-binding epidermal growth factor (HB-EGF), was also increased in the mutant uteri (fig. S10). In contrast, the expression of mRNAs of several other growth factor genes was either unaffected or slightly reduced in the *Hand2*-null uteri (fig. S10). We also observed that the uterine expression of *Fgf2*, *Fgf9*, and *Fgf18* progressively declined with the rise of *Hand2* expression as pregnancy advanced from day 1 to day 4 (fig. S11).

FGFs exert their paracrine responses through the cell surface FGF receptors (FGFRs) and a

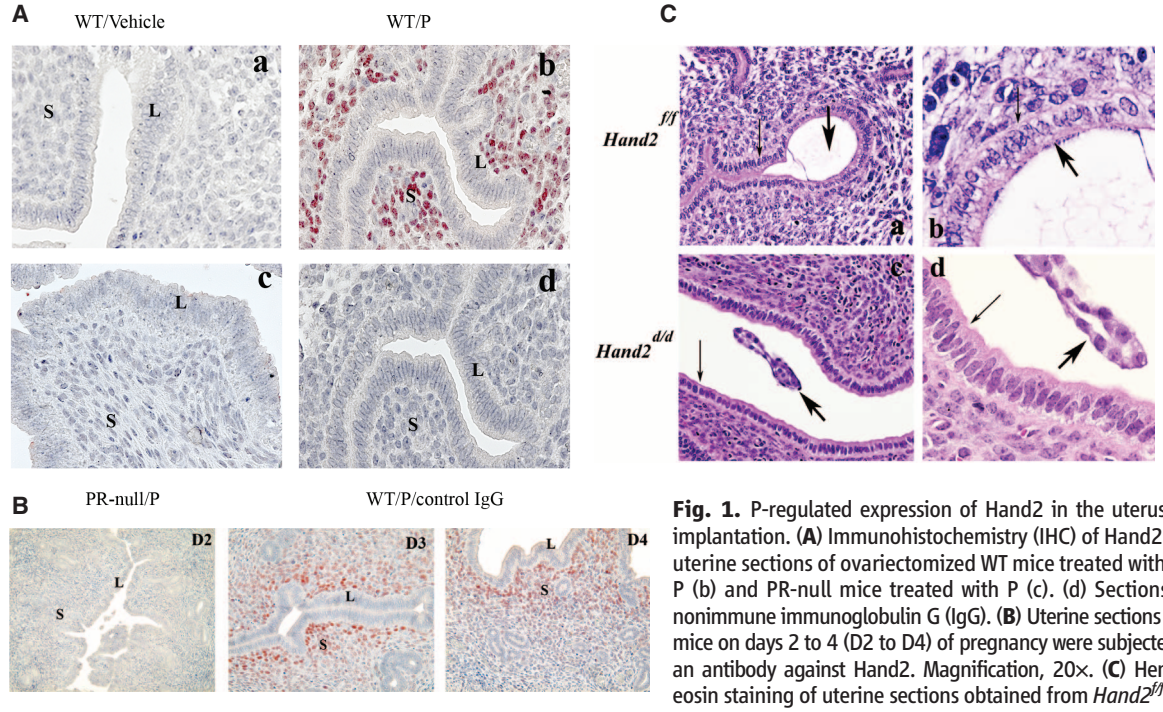

Fig. 1. P-regulated expression of Hand2 in the uterus is critical for implantation. (**A**) Immunohistochemistry (IHC) of Hand2 protein in the uterine sections of ovariectomized WT mice treated with vehicle (a) or P (b) and PR-null mice treated with P (c). (d) Sections treated with nonimmune immunoglobulin G (IgG). (**B**) Uterine sections obtained from mice on days 2 to 4 (D2 to D4) of pregnancy were subjected to IHC using an antibody against Hand2. Magnification, 20×. (**C**) Hematoxylin-and-eosin staining of uterine sections obtained from *Hand2*$^{f/f}$ (a and b) and *Hand2*$^{d/d}$ (c and d) mice on day 5 (n = 6) of pregnancy. (b) and (d) Magnified images of (a) and (c), respectively. Wide and narrow arrows point to embryo and luminal epithelium. L and S represent luminal epithelium and stroma, respectively.

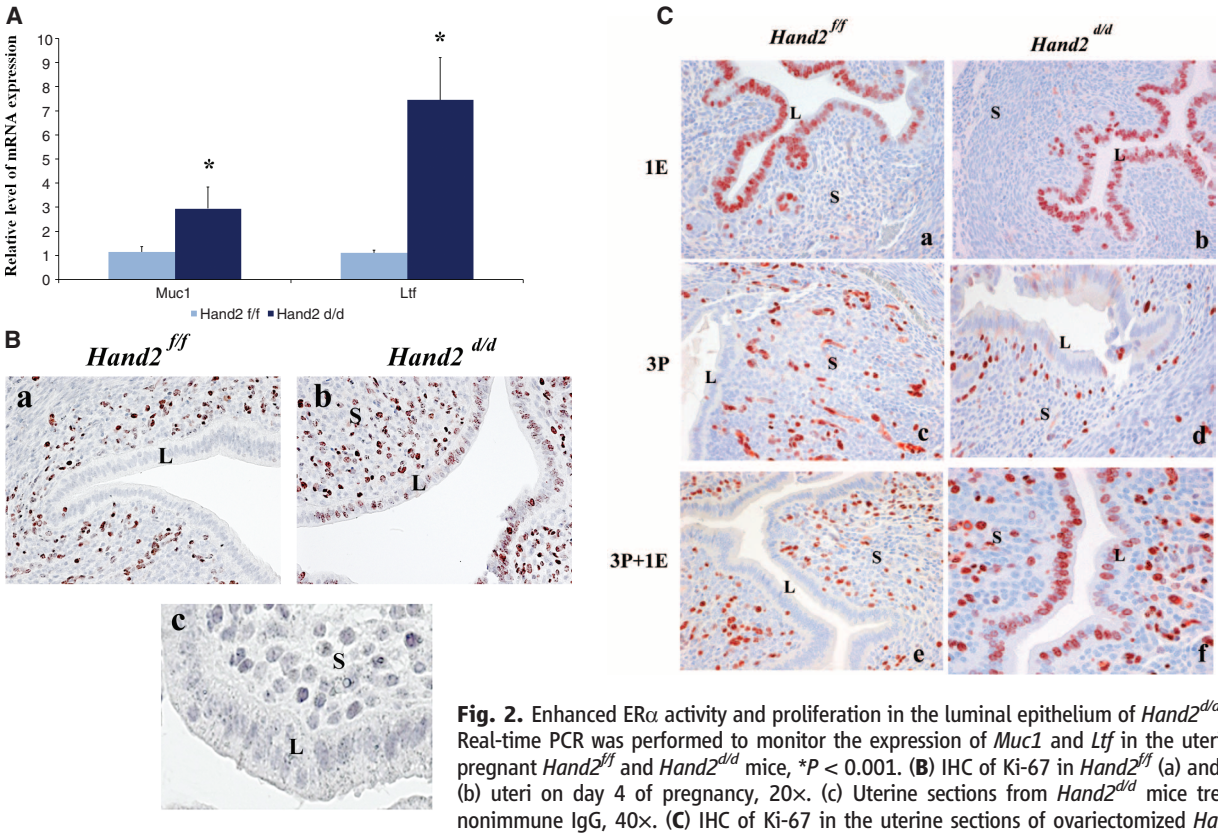

Fig. 2. Enhanced ERα activity and proliferation in the luminal epithelium of *Hand2*$^{d/d}$ uteri. (**A**) Real-time PCR was performed to monitor the expression of *Muc1* and *Ltf* in the uteri of day 4 pregnant *Hand2*$^{f/f}$ and *Hand2*$^{d/d}$ mice, *$P < 0.001$. (**B**) IHC of Ki-67 in *Hand2*$^{f/f}$ (a) and *Hand2*$^{d/d}$ (b) uteri on day 4 of pregnancy, 20×. (c) Uterine sections from *Hand2*$^{d/d}$ mice treated with nonimmune IgG, 40×. (**C**) IHC of Ki-67 in the uterine sections of ovariectomized *Hand2*$^{f/f}$ and *Hand2*$^{d/d}$ mice treated with E for 1 day (a) and (b), P for 3 days (c) and (d), or 2 days of P treatment followed by P and E (e) and (f).

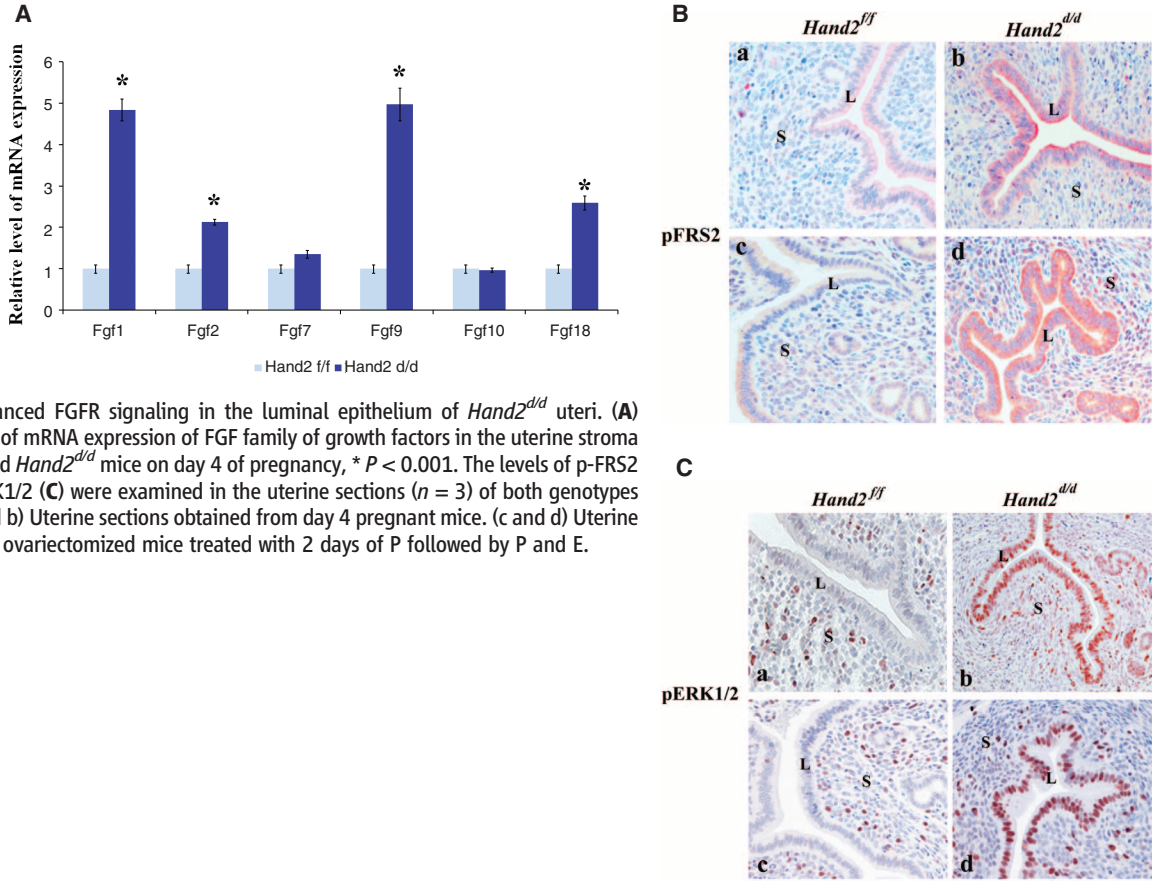

Fig. 3. Enhanced FGFR signaling in the luminal epithelium of *Hand2*$^{d/d}$ uteri. (**A**) Relative level of mRNA expression of FGF family of growth factors in the uterine stroma of *Hand2*$^{f/f}$ and *Hand2*$^{d/d}$ mice on day 4 of pregnancy, * $P < 0.001$. The levels of p-FRS2 (**B**) and p-ERK1/2 (**C**) were examined in the uterine sections ($n = 3$) of both genotypes by IHC. (a and b) Uterine sections obtained from day 4 pregnant mice. (c and d) Uterine sections from ovariectomized mice treated with 2 days of P followed by P and E.

docking protein complex (*14*). FGF-stimulation of FGFRs induces phosphorylation of specific tyrosine residues in a critical docking protein, FGFR substrate2 (FRS2), which guides the assembly of distinct multiprotein complexes, leading to activation of either extracellular signal–regulated kinase (ERK) 1 and 2 (ERK1/2) or phosphatidylinositol 3-kinase/Akt (PI3K/Akt) signaling cascades (*14*). We determined the expression of FGFRs 1 and 2 in uteri on days 1 and 4 of pregnancy and found that these receptors localized to the epithelium (fig. S12A). The levels of mRNAs corresponding to *Fgfr 1* to *3* were comparable in uteri of *Hand2*$^{f/f}$ and *Hand2*$^{d/d}$ mice on day 4 of pregnancy (fig. S12B).

The activation of the FGFR signaling pathway in uteri of *Hand2*$^{f/f}$ and *Hand2*$^{d/d}$ mice was monitored by examining the tyrosine phosphorylation status of FRS2. Whereas only low levels of phospho-FRS2 were seen in the uterine epithelium of *Hand2*$^{f/f}$ mice on day 4 of pregnancy (Fig. 3B, a), a marked increase in its level was observed in the epithelium of *Hand2*-null uteri, indicating that FGF signaling is activated in the absence of Hand2 (Fig. 3B, b). Phospho-FRS2 was undetectable in uterine epithelium of ovariectomized *Hand2*$^{f/f}$ mice in which P effectively blocks E-mediated proliferation (Fig. 3B, c). However, the epithelial cells of *Hand2*-null uteri, which showed proliferative activity under similar hormone treatment conditions, exhibited a marked elevation in the level of phospho-FRS2, reflecting the activation of FGFR signaling in these cells (Fig. 3B, d). We also monitored the activated phosphorylated states of ErbB1 and ErbB4, the primary receptors mediating the actions of *Hbegf* (*15*). The activated forms of these receptors were undetectable in uterine epithelia of *Hand2*$^{f/f}$ *and Hand2*$^{d/d}$ mice on day 4 of gestation (fig. S13), which indicated that the increased HB-EGF produced by the stroma of *Hand2*-null uteri did not act directly on the epithelial cells.

We next investigated whether the ERK1/2 and/or PI3K/Akt signaling pathways were activated downstream of FGFR in the epithelia of *Hand2*-ablated uteri. As shown in Fig. 3C, an increase in the level of phospho-ERK1/2 was seen in uterine epithelium of *Hand2*-null mice on day 4 of pregnancy (Fig. 3C, b) and also in response to E treatment in the presence of P (Fig. 3C, d). In contrast, the phospho-AKT levels were undetectable or low and remained unaltered in the uterine epithelia of these mice (fig. S14), which suggested that the ERK1/2 pathway, but not the PI3K/Akt pathway, is the key downstream mediator of enhanced FGF signaling in *Hand2*-null uteri.

To examine whether the elevated mitogenic activity in the luminal epithelium of *Hand2*$^{d/d}$ uteri is induced by FGF and ERK1/2 signaling, we administered PD173074 [a FGFR-specific inhibitor (*16*)] or vehicle into uterine horns of *Hand2*$^{d/d}$ mice at the time of implantation. The epithelia of vehicle-treated horn showed prominent expression of p-FRS2 and p-ERK1/2 (Fig. 4A, a and c). However, the levels of both p-FRS2 and p-ERK1/2 were reduced in the epithelia of PD173074-treated horn on day 4 of pregnancy (Fig. 4A, b and d). We also observed a marked decline in the proliferative activity of *Hand2*-null uterine epithelia, as indicated by decreased Ki-67 staining (Fig. 4A, e and f). In parallel experiments, administration of PD184352, an inhibitor of the ERK1/2 pathway (*17*), to uterine horns of *Hand2*$^{d/d}$ mice suppressed the level of pERK1/2 (Fig. 4B, a and b), as well as luminal epithelial

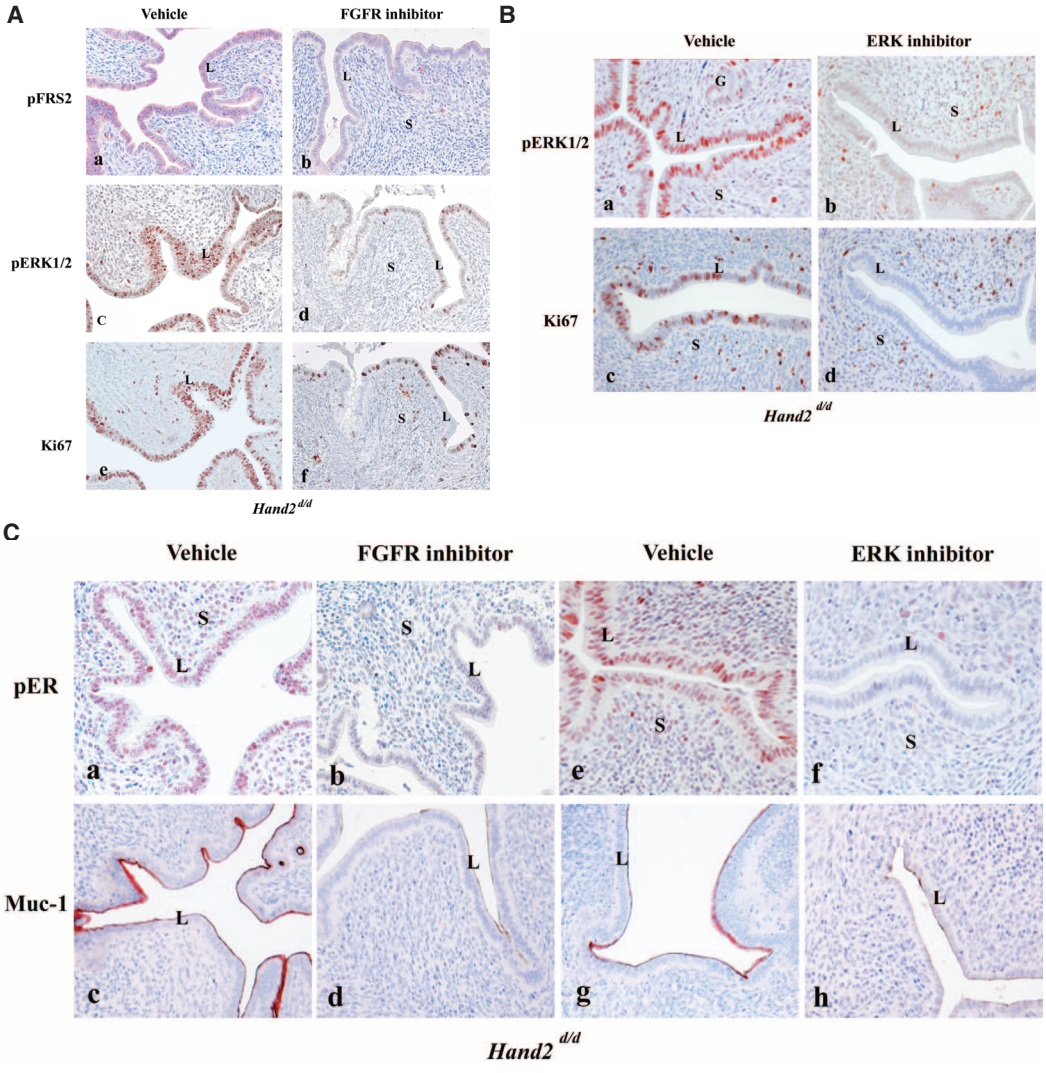

Fig. 4. The inhibitor PD173074 (**A**) or PD184352 (**B**) was administered to one uterine horn of Hand2$^{d/d}$ mice on day 3 of pregnancy (n = 5). The other horn served as vehicle-treated control. Uterine horns were collected on the morning of day 4, and sections were subjected to IHC to detect p-FRS2, p-ERK1/2, and Ki-67. (**C**) IHC of pERα and Muc-1 in uterine sections of Hand2$^{d/d}$ mice treated with PD173074 or PD184352.

proliferation (Fig. 4B, c and d). Collectively these results are consistent with the hypothesis that increased FGF production by the *Hand2*-null uterine stroma stimulates epithelial proliferation by activating the FGFR-ERK1/2 pathway.

The ERK1/2-dependent phosphorylation of epithelial ERα at Ser^{118} is critical for the transcriptional activation of ERα (*11*). Administration of either PD173074 (Fig. 4C, a to d) or PD184352 (Fig. 4C, e to h) to *Hand2*-null uterine horns blocked the phosphorylation of epithelial ERα at Ser^{118} and the expression of Muc-1. This result supported our view that elevated signaling by FGFR-ERK1/2 pathway in $Hand2^{d/d}$ uteri is responsible for phosphorylation and activation of ERα in epithelial cells, which promotes persistent expression of Muc-1 and which in turn creates a barrier that prevents embryo attachment.

Earlier studies using tissue recombinants prepared with uterine epithelium and stroma isolated from neonatal wild-type and PR-null mice indicated that the stromal PR plays an obligatory role in mediating the inhibitory actions of P on E-induced epithelial cell proliferation (*18*). However, the mechanism of this stromal-epithelial communication remained unknown. Our study has delineated a pathway in which Hand2 operates downstream of P to regulate the production of FGFs, mitogenic paracrine signals that originate in the stroma and act on the FGFR(s) in epithelium to control its E responsiveness (fig. S15). The antiproliferative action of P in uterine epithelium is of clinical significance, because the breakdown of this action underpins E-dependent endometrial cancer (*19*). Hand2, therefore, is an important factor to be considered for hormone therapy to block the proliferative actions of E in the endometrium.

References and Notes

1. C. A. Finn, L. Martin, *J. Reprod. Fertil.* **39**, 195 (1974).
2. D. D. Carson *et al.*, *Dev. Biol.* **223**, 217 (2000).
3. C. Y. Ramathal, I. C. Bagchi, R. N. Taylor, M. K. Bagchi, *Semin. Reprod. Med.* **28**, 17 (2010).
4. L. Martin, R. M. Das, C. A. Finn, *J. Endocrinol.* **57**, 549 (1973).
5. I. C. Bagchi, Y. P. Cheon, Q. Li, M. K. Bagchi, *Front. Biosci.* **8**, s852 (2003).
6. H. Pan, Y. Deng, J. W. Pollard, *Proc. Natl. Acad. Sci. U.S.A.* **103**, 14021 (2006).
7. I. C. Bagchi *et al.*, *Semin. Reprod. Med.* **23**, 38 (2005).
8. D. Srivastava *et al.*, *Nat. Genet.* **16**, 154 (1997).
9. A. B. Firulli, *Gene* **312**, 27 (2003).
10. Materials and methods are available as supporting material on *Science* Online.
11. S. Kato *et al.*, *Science* **270**, 1491 (1995).
12. G. A. Surveyor *et al.*, *Endocrinology* **136**, 3639 (1995).
13. K. Y. Lee *et al.*, *Nat. Genet.* **38**, 1204 (2006).
14. V. P. Eswarakumar, I. Lax, J. Schlessinger, *Cytokine Growth Factor Rev.* **16**, 139 (2005).
15. R. Iwamoto, E. Mekada, *Cytokine Growth Factor Rev.* **11**, 335 (2000).
16. M. Koziczak, T. Holbro, N. E. Hynes, *Oncogene* **23**, 3501 (2004).
17. D. B. Solit *et al.*, *Nature* **439**, 358 (2006).
18. T. Kurita *et al.*, *Endocrinology* **139**, 4708 (1998).
19. J. J. Kim, E. Chapman-Davis, *Semin. Reprod. Med.* **28**, 81 (2010).

20. We thank M. Laws for genotyping and Y. Li for immunohistochemistry. This work was supported by the Eunice Kennedy Shriver National Institute of Child Health and Human Development, NIH, through U54HD055787 as part of the Specialized Cooperative Centers Program in Reproduction and Infertility Research. The Gene Expression Omnibus (GEO) microarray accession number is GSE25881.

Supporting Online Material

www.sciencemag.org/cgi/content/full/331/6019/912/DC1
Materials and Methods
Figs. S1 to S15
Table S1
References

7 September 2010; accepted 15 December 2010
10.1126/science.1197454

Distinct Properties of the XY Pseudoautosomal Region Crucial for Male Meiosis

Liisa Kauppi,[1] Marco Barchi,[2,3] Frédéric Baudat,[2]* Peter J. Romanienko,[2] Scott Keeney,[1,4]† Maria Jasin[2]†

Meiosis requires that each chromosome find its homologous partner and undergo at least one crossover. X-Y chromosome segregation hinges on efficient crossing-over in a very small region of homology, the pseudoautosomal region (PAR). We find that mouse PAR DNA occupies unusually long chromosome axes, potentially as shorter chromatin loops, predicted to promote double-strand break (DSB) formation. Most PARs show delayed appearance of RAD51/DMC1 foci, which mark DSB ends, and all PARs undergo delayed DSB-mediated homologous pairing. Analysis of *Spo11*β isoform–specific transgenic mice revealed that late RAD51/DMC1 foci in the PAR are genetically distinct from both early PAR foci and global foci and that late PAR foci promote efficient X-Y pairing, recombination, and male fertility. Our findings uncover specific mechanisms that surmount the unique challenges of X-Y recombination.

Meiotic recombination, initiated by programmed double-strand breaks (DSBs), promotes homologous chromosome (homolog) pairing during prophase I (*1*). A subset of DSBs matures into crossovers that physically connect homologs so that they orient properly on the first meiotic spindle. Because sex chromosome recombination and pairing are restricted to the PAR (*2*), at least one DSB must form within this small region, and the homologous PAR must be located and engaged in recombination to lead to a crossover. Accordingly, the PAR in males exhibits high crossover frequency (*2*, *3*), but sex chromosomes also missegregate more frequently than autosomes (*4*). Nevertheless, X-Y nondisjunction is rare, which suggests that there are mechanisms that ensure successful X-Y recombination.

X-Y pairing is more challenging than autosomal pairing, as it cannot be mediated by multiple DNA interactions along the length of the chromosomes. We used fluorescence in situ hybridization (FISH) (*5*) to compare timing of meiotic X-Y and autosomal pairing in mice (Fig. 1). At leptonema, when DSBs begin to form and only short chromosome axis segments are present, PAR and autosomal FISH probes were mostly unpaired. By early to mid-zygonema, when axes elongate and homologs become juxtaposed, distal ends of chr 18 and 19 were paired in ~50% of nuclei; by late zygonema, these regions were paired in nearly all nuclei (Fig. 1B and fig. S1). In contrast, the X and Y PARs were rarely paired before pachynema (Fig. 1B); hence, X-Y pairing is delayed compared with that of autosomes.

DSBs precede and are required for efficient homolog pairing in mouse meiosis (*6*, *7*). Nucleus-wide ("global") foci of DSB markers RAD51/DMC1 peak in number at early to mid-zygonema (Fig. 2A) (*8*, *9*). Because stable X-Y pairing occurs late, we asked whether PAR DSB kinetics is also delayed (Fig. 2B and fig. S2). More than half of cells had no RAD51/DMC1 focus in the PAR before late zygonema (Fig. 2C), distinct from global patterns. Only when global foci were already declining did the majority of cells (~70%) display PAR foci (Fig. 2C and fig. S2*i*). We interpret the lack of PAR foci to indicate that DSBs have not yet formed. Thus, we propose that PAR DSB formation and/or turnover are under distinct temporal control. We cannot exclude the alternative possibility that PAR DSBs have formed but are cytologically undetectable, for example, because RAD51/DMC1 have not yet been loaded onto DSB ends or because foci have already turned over. In either case, DSB dynamics and/or processing differs on the PAR.

Most sites marked by PAR RAD51/DMC1 foci appeared incapable of mediating stable pairing before early pachynema (~70% of late zygotene

[1]Molecular Biology Program, Memorial Sloan-Kettering Cancer Center, New York, NY 10065, USA. [2]Developmental Biology Program, Memorial Sloan-Kettering Cancer Center, New York, NY 10065, USA. [3]Department of Public Health and Cell Biology, Section of Anatomy, University of Rome Tor Vergata, 00133 Rome, Italy. [4]Howard Hughes Medical Institute, Memorial Sloan-Kettering Cancer Center, New York, NY 10065, USA.

*Present address: Institute of Human Genetics, CNRS, 34090 Montpellier, France.

†To whom correspondence should be addressed. E-mail: m-jasin@ski.mskcc.org (M.J.); s-keeney@ski.mskcc.org (S.K.)